Adipose Deficiency of *Nrf2* in *ob/ob* Mice Results in Severe Metabolic Syndrome

Peng Xue,[1] Yongyong Hou,[1] Yanyan Chen,[1,2] Bei Yang,[1,3] Jingqi Fu,[1] Hongzhi Zheng,[1,2] Kathy Yarborough,[1] Courtney G. Woods,[1] Dianxin Liu,[4] Masayuki Yamamoto,[5] Qiang Zhang,[1] Melvin E. Andersen,[1] and Jingbo Pi[1]

Nuclear factor E2–related factor 2 (Nrf2) is a transcription factor that functions as a master regulator of the cellular adaptive response to oxidative stress. Our previous studies showed that Nrf2 plays a critical role in adipogenesis by regulating expression of CCAAT/enhancer-binding protein β and peroxisome proliferator–activated receptor γ. To determine the role of Nrf2 in the development of obesity and associated metabolic disorders, the incidence of metabolic syndrome was assessed in whole-body or adipocyte-specific *Nrf2*-knockout mice on a leptin-deficient *ob/ob* background, a model with an extremely positive energy balance. On the *ob/ob* background, ablation of *Nrf2*, globally or specifically in adipocytes, led to reduced white adipose tissue (WAT) mass, but resulted in an even more severe metabolic syndrome with aggravated insulin resistance, hyperglycemia, and hypertriglyceridemia. Compared with wild-type mice, WAT of *ob/ob* mice expressed substantially higher levels of many genes related to antioxidant response, inflammation, adipogenesis, lipogenesis, glucose uptake, and lipid transport. Absence of *Nrf2* in WAT resulted in reduced expression of most of these factors at mRNA or protein levels. Our findings support a novel role for Nrf2 in regulating adipose development and function, by which Nrf2 controls the capacity of WAT expansion and insulin sensitivity and maintains glucose and lipid homeostasis. ***Diabetes*** 62:845–854, 2013

W hite adipose tissue (WAT) is an active organ that can store and release energy, maintain lipid and glucose homeostasis, and secrete a variety of factors that influence appetite, insulin sensitivity, inflammation, and many other pathways of biological and clinical significance (1). Excess accumulation of WAT is a risk factor for insulin resistance and type 2 diabetes. Conversely, defects in adipogenesis or lipogenesis in WAT as in lipodystrophy, which impair the capacity of WAT to expand, also can result in insulin resistance (2,3).

Nuclear factor E2–related factor 2 (Nrf2, also known as Nfe2l2) is a master regulator of the cellular adaptive response to oxidative stress (4–6). In response to oxidative

and electrophilic stress, Nrf2 heterodimerizes with small Maf proteins and other basic leucine zipper proteins and binds to antioxidant response elements (AREs) in the promoters of many antioxidant and detoxification genes (7), thereby increasing their transcription. Evidence supporting the pivotal roles of Nrf2 in protecting against oxidative stress comes, in part, from studies conducted in *Nrf2*-knockout ($Nrf2^{-/-}$) mice that revealed that these animals exhibit a severe deficiency in the coordinated gene regulatory program for adaptive antioxidant response resulting in high susceptibility to oxidative stress-related disorders and chemical carcinogenesis (8). Thus, the Nrf2-mediated antioxidant response represents an important cellular defense mechanism that serves to maintain intracellular redox homeostasis and to limit oxidative damage (5,9). In addition to liver, intestine, lung, and kidney, where detoxification reactions routinely occur (10), Nrf2 is abundantly expressed or highly inducible in human and mouse adipocytes and in WAT (11,12). However, other than detoxification and antioxidant defense, the exact function of Nrf2 in adipose tissues is not well-understood.

Our previous study (11) showed that mice deficient in *Nrf2* possess decreased fat mass and are resistant to high-fat diet–induced obesity. In addition, we found that Nrf2 serves as an important transcriptional regulator of CCAAT/ enhancer-binding protein β (C/EBPβ) (12) and peroxisome proliferator–activated receptor γ (PPARγ) (11) during adipocyte differentiation, suggesting that Nrf2 is one of the key transcription factors that controls adipogenesis. Defects in adipogenesis (e.g., caused by ablation of *Pparγ* or suppression of C/EBP) are critical pathogenic factors of lipodystrophy, a syndrome characterized by total or partial fat loss associated with severe lipid and glucose abnormalities leading to diabetes with early cardiovascular, renal, and hepatic complications (13–15). To examine the role of Nrf2 in adipose function and metabolic syndrome, in the current study we determined the effect of ablation of *Nrf2* on the development of obesity and associated metabolic disorders in leptin-deficient (*ob/ob*) mice, a model with an extremely positive energy balance. Interestingly, *ob/ob* mice with whole-body or adipocyte-specific ablation of *Nrf2* displayed reduced WAT mass but had an even more severe metabolic syndrome characterized by hyperlipidemia, aggravated insulin resistance, and hyperglycemia. These findings provide further support that Nrf2 is a key transcription factor that controls WAT development and function, and thus affects insulin sensitivity, glucose tolerance, and lipid homeostasis. In light of the new function of Nrf2 in adipogenesis and its canonical role in adaptive antioxidant response, our results suggest a novel mechanistic linkage between metabolic syndrome and oxidative stress, opening the possibility that manipulation

of Nrf2 may prevent or treat obesity and associated metabolic syndrome.

RESEARCH DESIGN AND METHODS

Mice. Global Nrf2$^{-/-}$ mice were developed as described previously (10) and back-crossed onto the C57BL/6J background for seven generations using alternating male and female stock mice from The Jackson Laboratories (JAX Stock No. 000664). The resulting Nrf2$^{+/-}$ females were crossed with heterozygous male B6.V-Lep^{ob}/J mice (ob/−, JAX Stock No. 000632) to generate Nrf2$^{+/-}$:ob/− mice, which were used to breed Nrf2$^{-/-}$:ob/ob and Nrf2$^{+/+}$:ob/ob mice for the current study. To delete Nrf2 only in adipocytes, a line of C57BL/6J mice in which exon 5 of the Nrf2 gene was flanked by LoxP sites (Nrf2$^{LoxP/LoxP}$) was generated as detailed in Supplementary Fig. 1A. The Nrf2$^{LoxP/LoxP}$ mice were crossed with mice expressing Cre recombinase under the control of the adipocyte-specific Fabp4/aP2 gene promoter [B6.Cg-Tg(Fabp4-cre)1Rev/J; JAX Stock No. 005069]. The resulting adipocyte-specific Nrf2$^{-/-}$ mice [Nrf2 (f)$^{-/-}$], with the genotype of Nrf2$^{LoxP/LoxP}$:Cre$^{+/+}$ or Cre$^{+/-}$, lacked Nrf2 expression in WAT and brown adipose tissues, but not in liver, skeletal muscle, pancreas, or lung (Supplementary Fig. 1B). Subsequently, the Nrf2(f)$^{-/-}$ mice were crossed with ob/− mice to generate Nrf2(f)$^{-/-}$:ob/ob and Nrf2(f)$^{+/+}$:ob/ob mice. The mice were housed in virus-free facilities on a 12-h light/12-h dark cycle and were fed NIH07 chow diet (Zeigier Brothers, Gardners, PA) and provided reverse-osmosis water ad libitum. Body weight and food consumption were determined weekly to allow calculation of cumulative food consumption. Genotyping was performed by PCR (primer sequences in Supplementary Table 1) using genomic DNA that was isolated from tail snips. All protocols for animal use were approved by the Institutional Animal Care and Use Committee of The Hamner Institutes and were in accordance with the National Institutes of Health guidelines.

Measurements of fasting blood glucose and plasma insulin. After a 16-h period, fasting blood samples collected from tail bleeds were immediately analyzed for glucose using the FreeStyle Blood Glucose Monitoring System (TheraSense, Alameda, CA). Animals for plasma isolation and tissue collection were euthanized by CO$_2$ exposure and exsanguinations. Plasma for the insulin assay was filtered using an YM-100 Microcon centrifugal filter (Millipore, Billerica, MA) to remove hemoglobin contamination. Plasma insulin was measured with the Sensitive Rat Insulin radioimmunoassay kit (SRI-13K; EMD Millipore, Billerica, MA) as described previously (16). The homeostatic model assessment for insulin resistance was determined by performing the following calculation: homeostatic model assessment for insulin resistance = fasting plasma insulin (mU/L) × fasting blood glucose (mg/dL)/405.

Intraperitoneal glucose tolerance test and intraperitoneal insulin tolerance test. Intraperitoneal glucose tolerance test and intraperitoneal insulin tolerance test were performed as described previously (16). Briefly, after 16 h fasting animals received D-(+)-glucose (0.5 g/kg body weight [BW]; G8769; Sigma, St. Louis, MO) or insulin (0.75 U/kg BW for non-ob/ob mice; 4 U/kg BW for ob/ob mice; I9278; Sigma) by intraperitoneal injection. At 15, 30, 60, and 120 min after glucose or insulin administration, glucose levels in blood collected from tail bleeds were analyzed immediately as detailed.

Lipid measurements in plasma and tissues. Triglycerides and free glycerol in plasma were determined in duplicate using the Triglycerides Assay Kit (TR0100; Sigma, St. Louis, MO). Plasma free fatty acids were assessed in triplicate using the colorimetric assays (Zen-Bio, Chapel Hill, NC). Tissue samples (10 mg each) for triglycerides measurement were homogenized in 100 μL of the Lipid Extraction Solution (K610-100; Biovision, Mountain View, CA) for 5 min with TissueLyser II (Retsch, Newtown, PA). The homogenates were heated at 95°C for 30 min and mixed vigorously for 1 min, followed by centrifuging (12,000g, 5 min), and the resulting supernatants were used for the assay.

Histology and immunostaining. The liver, WAT, and brown adipose tissue were fixed, embedded in paraffin, sectioned, and stained with hemotoxylin and eosin or immunofluorescent staining as described previously (16). For immunofluorescent staining, slides were blocked in 1.5% blocking serum in PBS for 1 h and subsequently incubated overnight at 4°C with the antiglucose transporter type 4 (GLUT4, mouse IgG1, 2213, 1:200; Cell Signaling Technology, Danvers, MA) diluted in 1.5% blocking serum in PBS. After rinsing in PBS, the slides were incubated with goat anti-mouse IgG-FITC secondary antibody (62-6311, 1:50; ZYMED Laboratories, South San Francisco, CA). After DAPI staining, the slides were mounted, covered with coverslips, and examined using an Axio Observer Z1 fluorescence microscope (Carl Zeiss, Oberkochen, Germany). The concentrations of primary and secondary antibodies for immunostaining were determined by antibody titrations. All sections were blindly scored by pathologists at The Hamner Institutes.

Measurement of glutathione. Levels of total glutathione and oxidized glutathione (GSSG) in whole blood and plasma were measured immediately after sample collection using the BIOXYTECH GSH/GSSG-412 kit (OxisResearch, Portland, OR) as described previously (16). Samples for GSSG measurement were immediately mixed with the thiol-scavenging reagent 1-methyl-2-vinyl-pyridium trifluoromethane sulfonate after separation. The concentrations of reduced glutathione (GSH) were calculated by the equation: GSH = total glutathione − (2 × GSSG).

Reverse-transcription quantitative real-time PCR (RT-qPCR). Total RNA in WAT and liver was isolated with TRIzol (Invitrogen) using the TissueLyser II and subsequently subjected to clean-up using an RNase-Free DNase Set and RNeasy Mini kit (Qiagen, Valencia, CA). The resultant DNA-free RNA samples were stored at −80°C until use. Total RNA was reverse-transcribed with MuLV reverse-transcriptase and Oligo d(T) primers (Applied Biosystems, Foster City, CA). A SensiFAST SYBR Hi-ROX kit (BIOLINE USA, Taunton, MA) was used for quantitative PCR. The primers were designed using Primer Express 4 (Applied Biosystems) and synthesized by Bioneer (Alameda, CA). The primer sequences are listed in Supplementary Table 3. Relative differences in gene expression among groups were determined from quantification cycle (C$_q$) values. These values were first normalized to 18 ribosomal RNA (18S) in the same sample (ΔC$_q$) and expressed as the fold-change over control (2$^{-\Delta\Delta C_q}$). Real-time fluorescence detection was performed using an ABI PRISM 7900HT Fast Real-time PCR System (Applied Biosystems). Details on the procedures of RNA quantification and reverse-transcription quantitative PCR are described in the Supplemental Materials.

Immunoblot analysis. Tissue lysates of WAT were prepared according to the P2-B&D protocol developed by Sajic et al. (17) (details in the Supplemental Materials). Resulting tissue lysates were used for immunoblot analysis as detailed previously (18). Antibodies for PPARγ (2435; 1:1,000), GLUT4 (2213; 1:1,000), p-AKT(T308) (2965; 1:1,000), p-AKT(S473) (9271; 1:1,000), and AKT (4691; 1:1,000) were purchased from Cell Signaling Technology (Danvers, MA). Antibodies for β-actin (A1978; 1:2,000) and glyceraldehyde 3-phosphate dehydrogenase (sc-20357; 1:1,000) were purchased from Sigma-Aldrich (St. Louis, MO) and Santa Cruz Biotechnology (Santa Cruz, CA), respectively. The molecular weight of each protein shown on the immunoblot was estimated based on the MagicMark XP Western Protein Standard (Invitrogen) on 12% Tris-Glycine gels (Invitrogen). Quantification of the results was performed by Bio-Rad Quantity One one-dimensional analysis software (Bio-Rad Laboratories, Hercules, CA).

Statistical analysis. All statistical analysis was performed using Graphpad Prism 4 (GraphPad Software, San Diego, CA), with P < 0.05 considered as significant. More specific indices of statistical significance are indicated in individual figure legends. Data are expressed as mean ± SD. For comparisons between two groups, a Student t test was performed. For comparisons among groups, one-way or two-way ANOVA with Bonferroni post hoc testing was performed.

RESULTS

Global ablation of Nrf2 in ob/ob mice reduces body mass but aggravates insulin resistance and hyperglycemia. The BW of Nrf2$^{-/-}$:ob/ob, WT ob/ob (Nrf2$^{+/+}$:ob/ob), and their non-ob/ob littermates (Nrf2$^{-/-}$:WT or Nrf2$^{+/+}$:WT) was monitored during an 11-week period in mice 4–15 weeks of age. On a normal chow diet, Nrf2$^{-/-}$:ob/ob mice gained weight at a lower rate than Nrf2$^{+/+}$:ob/ob mice, such that they weighed substantially less from week 5 through week 11. Maximal differences were observed during week 8, at which time the body mass of the Nrf2$^{-/-}$:ob/ob mice was less than that of Nrf2$^{+/+}$:ob/ob mice by 23% in males (Fig. 1A) and by 26% in females (Supplementary Fig. 2A), respectively. Cumulative food consumption by Nrf2$^{-/-}$:ob/ob mice showed a similar rate as in Nrf2$^{+/+}$:ob/ob mice up to week 10 (Fig. 1B), but gradually decreased beyond this time point in females (Supplementary Fig. 2B). Compared with Nrf2$^{+/+}$:ob/ob mice, both male and female Nrf2$^{-/-}$:ob/ob mice had development of hyperglycemia and trended toward an increase in fasting plasma insulin and homeostatic model assessment for insulin resistance (Fig. 1C–E and Supplementary Fig. 2C–E). In addition, Nrf2$^{-/-}$:ob/ob mice exhibited insulin resistance demonstrated by a severely blunted response to intraperitoneal glucose tolerance test (Fig. 1F and Supplementary Fig. 2F) and intraperitoneal insulin tolerance test (Fig. 1G and Supplementary Fig. 2G).
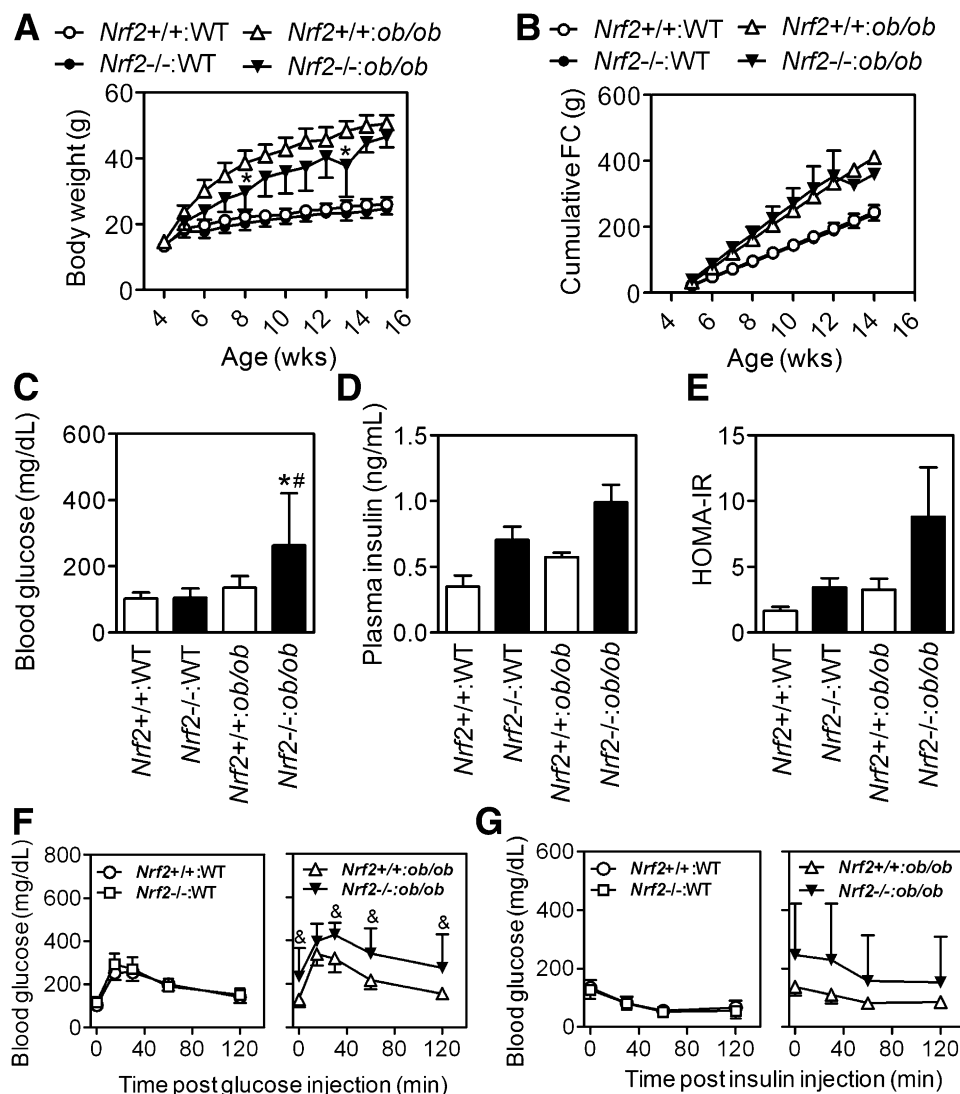
FIG. 1. *Ob/ob* male mice with global *Nrf2* deletion exhibit reduced BW, aggravated insulin resistance, and hyperglycemia. *A*: BW analysis of mice maintained on a chow diet. $n = 8–11$. *$P < 0.05$ vs. $Nrf2^{+/+}$:ob/ob mice at the same age. *B*: Cumulative food consumption. $n = 3–8$. *C*: Fasting blood glucose. $n = 16–29$. *$P < 0.05$ vs. non-*ob/ob* mice with the same *Nrf2* genotype; #$P < 0.05$ vs. $Nrf2^{+/+}$:ob/ob mice. *D*: Fasting plasma insulin. $n = 3–5$. *E*: Homeostatic model assessment for insulin resistance (HOMA-IR). $n = 3–5$. *F*: Intraperitoneal glucose tolerance test. Mice were challenged with 0.5 mg of glucose per gram of BW. $n = 7–9$. &$P < 0.05$ vs. $Nrf2^{+/+}$:ob/ob mice with the same treatment. *G*: Intraperitoneal insulin tolerance test. Mice were challenged with insulin at 0.75 and 4 U/g of BW in non-*ob/ob* and *ob/ob* mice, respectively. $n = 8–15$.

Of note, four of 34 $Nrf2^{-/-}$:ob/ob mice died between 8 and 12 weeks because of severe metabolic disorders exhibiting extraordinary hyperglycemia (>499 mg/dL), dark yellow urine, and very low BW. Consistent with previous reports (11,19), $Nrf2^{-/-}$:WT mice fed normal chow diet displayed slightly reduced BW gain, normal fasting blood glucose level, and insulin sensitivity compared with $Nrf2^{+/+}$:WT mice (Fig. 1*A* and Supplementary Fig. 2).

Global ablation of *Nrf2* in *ob/ob* mice reduces WAT mass and alleviates hepatic steatosis, but results in hypertriglyceridemia. Although $Nrf2^{-/-}$:ob/ob mice still had development of adipose (Fig. 2*A*) and their visceral WAT pads, including retroperitoneal and epididymal (male) or gonadal (female) depots, were significantly smaller than those of $Nrf2^{+/+}$:ob/ob mice (Fig. 2*B* and Supplementary Fig. 3*A*). Histomorphometric analysis of WAT displayed that $Nrf2^{-/-}$:ob/ob mice had fewer small adipocytes in subcutaneous and epididymal WAT than $Nrf2^{+/+}$:ob/ob mice (Fig. 2*C* and Supplementary Fig. 4), suggesting that deficiency of

Nrf2 impairs the capability of adipocyte recruitment (20). Interestingly, $Nrf2^{-/-}$:ob/ob mice were protected against hepatic steatosis, showing notably less accumulation of hepatic lipid droplets as well as smaller lipid droplet size than $Nrf2^{+/+}$:ob/ob mice (Fig. 2*C*). In addition, $Nrf2^{-/-}$:ob/ob mice displayed a substantially reduced intrahepatic triglyceride content (Fig. 2*D* and Supplementary Fig. 3*B*). In contrast to the reduced lipid deposition in liver, $Nrf2^{-/-}$:ob/ob mice exhibited a trend toward hypertriglyceridemia, with a nearly 52.6% (males) and 39.6% (females) increase of fasting plasma triglyceride levels compared with $Nrf2^{+/+}$:ob/ob mice (Fig. 2*E* and Supplementary Fig. 3*C*). When the data in males and females were pooled, a significant difference of plasma triglycerides levels between $Nrf2^{+/+}$:ob/ob and $Nrf2^{-/-}$:ob/ob mice was reached (not shown). Triglycerides in the skeletal muscle (Fig. 2*F*, Supplementary Fig. 3*D*) and plasma levels of free glycerol and free fatty acids (Supplementary Fig. 5) showed no significant difference between $Nrf2^{+/+}$:ob/ob and $Nrf2^{-/-}$:ob/ob mice.
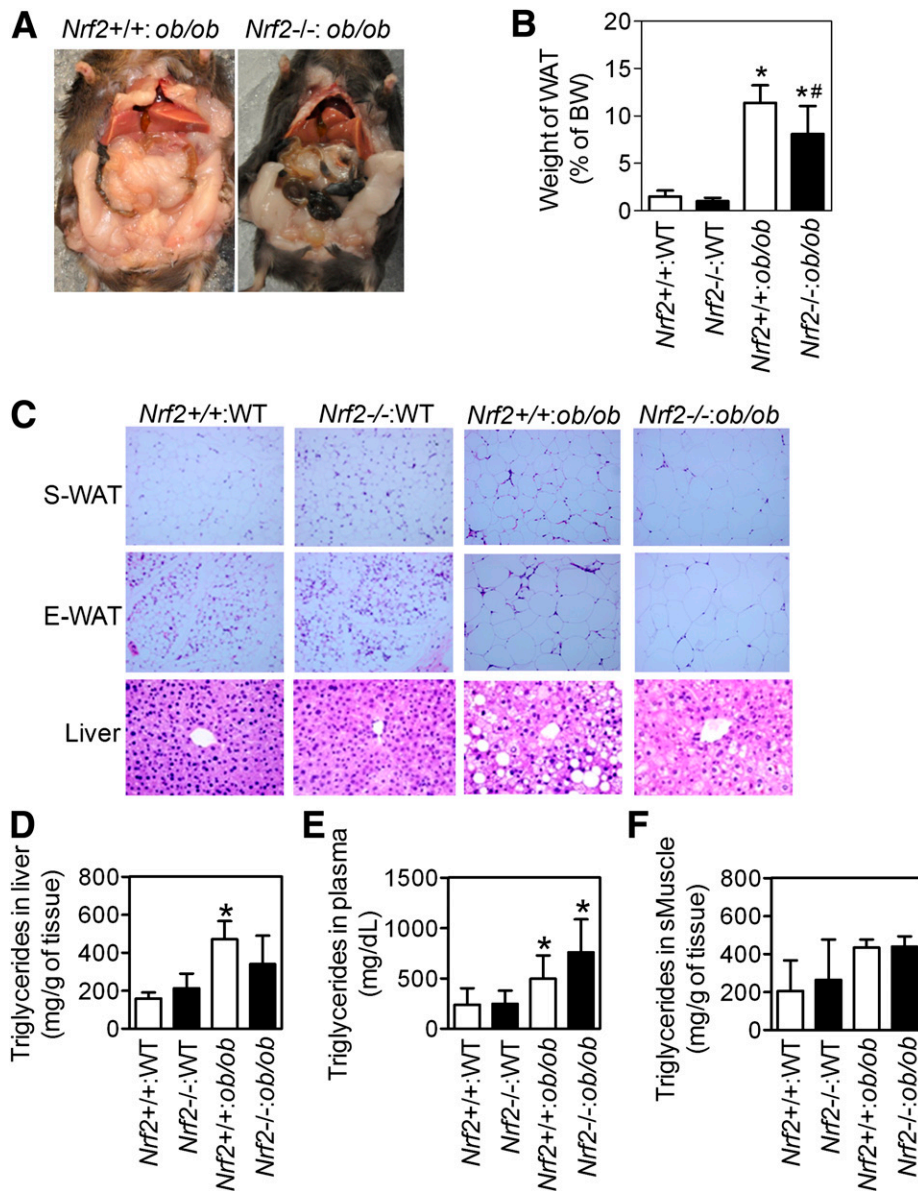
FIG. 2. Nrf2$^{-/-}$:ob/ob male mice show reduced WAT mass and mild hepatic steatosis but trended increased plasma triglycerides. A: Representative images of fat tissues. Animal age is 10 weeks. B: Weight of WAT. Retroperitoneal and epididymal depots were measured. n = 11–18. Animal age is 8–15 weeks. C: Representative histological images of WAT and liver with hematoxylin and eosin (H&E) staining (20×). S-WAT, subcutaneous WAT; E-WAT, epididymal WAT. The white round areas on liver slides are lipid droplets. D–F: Levels of triglycerides in liver (D), plasma (E), and skeletal muscle (sMuscle) (F) are shown. n = 6–7. Values in B, D, E, and F are mean ± SD. *P < 0.05 vs. non-ob/ob mice with the same Nrf2 genotype; #P < 0.05 vs. Nrf2$^{+/+}$:ob/ob mice. (A high-quality color representation of this figure is available in the online issue.)

Ob/ob mice with adipocyte-specific Nrf2 knockout exhibit a similar phenotype as Nrf2$^{-/-}$:ob/ob mice showing reduced WAT mass, increased plasma triglycerides, insulin resistance, and hyperglycemia. A reduction in fat, commonly found in genetically engineered mouse models, could be attributable to a number of biochemical abnormalities in other tissues. To substantiate a regulatory role of Nrf2 in adipose function and glucose homeostasis, a line of ob/ob mice with adipocyte-specific Nrf2 deletion was developed (Supplementary Fig. 1). The adipocyte-specific knockout of Nrf2 in ob/ob mice resulted in significantly diminished expression of Nrf2 in WAT (Fig. 3A). In agreement with the findings in Nrf2$^{-/-}$:ob/ob mice, Nrf2(f)$^{-/-}$:ob/ob mice fed a chow diet showed a trend toward decreased BW (Fig. 3B) and significantly reduced WAT mass (Fig. 3C). Histomorphometric analysis

of WAT demonstrated a trend in which Nrf2$^{-/-}$(f):ob/ob mice had fewer small adipocytes in epididymal WAT than Nrf2$^{+/+}$(f):ob/ob mice (Supplementary Fig. 6). Consistent with the phenotype of Nrf2$^{-/-}$:ob/ob mice, Nrf2(f)$^{-/-}$:ob/ob mice exhibited significantly increased plasma triglycerides (Fig. 3F), reduced insulin sensitivity (Fig. 3G and H), and elevated fasting blood glucose levels (Fig. 3I). Thus, the severe metabolic syndrome of Nrf2$^{-/-}$:ob/ob mice remains in Nrf2(f)$^{-/-}$:ob/ob mice, and the phenotype of Nrf2 deletion in ob/ob mice can be attributed, at least in part, to the lack of Nrf2 in adipose tissues. In contrast to the reduced lipid content in the liver of Nrf2$^{-/-}$:ob/ob mice (Fig. 2C and D), adipocyte-specific ablation of Nrf2 did not significantly affect lipid deposition in the liver or skeletal muscle (Fig. 3D and E).
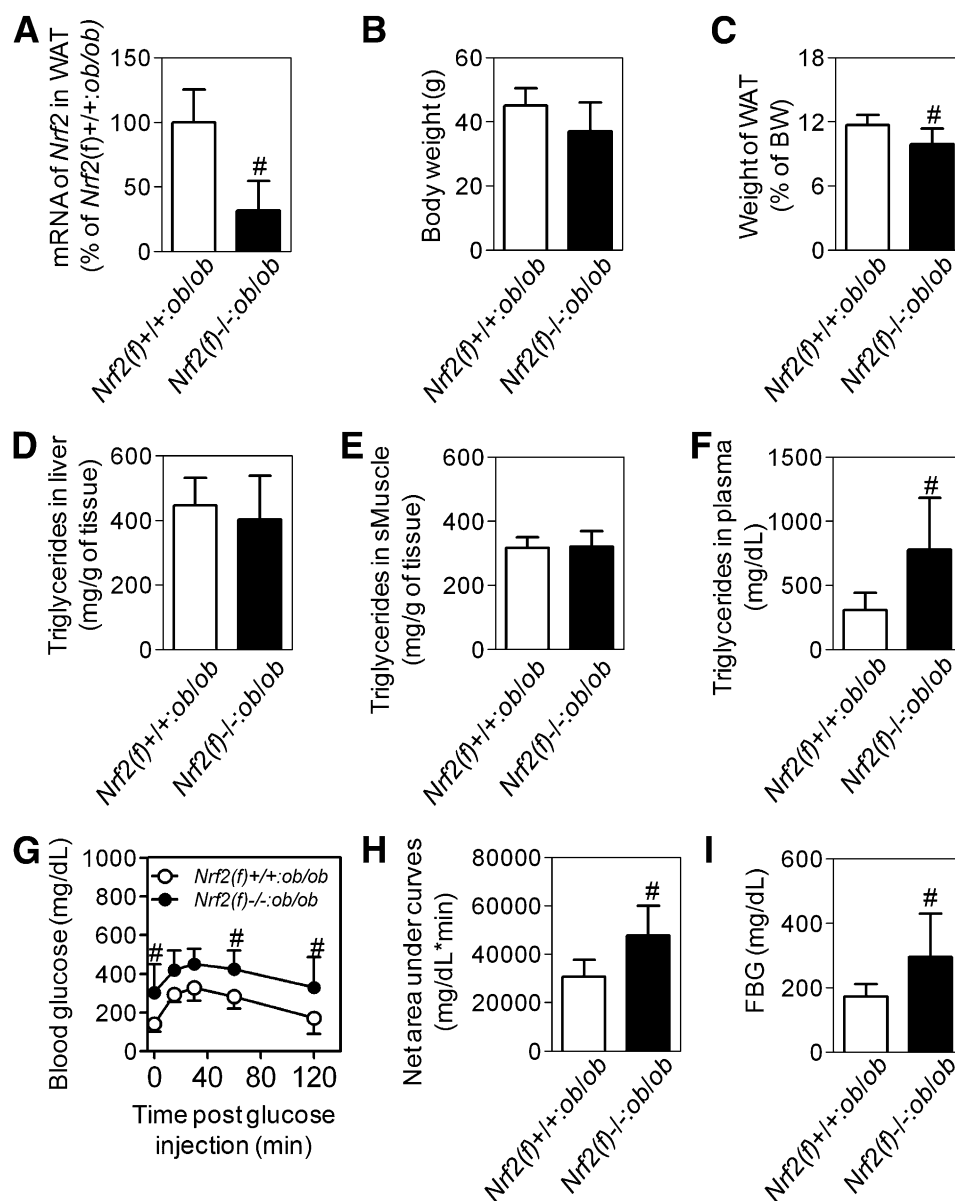
FIG. 3. Adipocyte-specific ablation of *Nrf2* in o*b/ob* mice results in reduced WAT mass, hyperlipidemia, aggravated insulin resistance, and hyperglycemia. *A*: Gene expression of *Nrf2* in WAT. $n = 3–4$ males. *B*: Body weight of mice maintained on a chow diet. *C*: Weight of WAT. *D–F*: Triglycerides in liver (*D*), skeletal muscle (sMuscle) (*E*), and plasma (*F*) of mice with 16-h fasting. *G*: Intraperitoneal glucose tolerance test. Mice were challenged with 0.5 mg of glucose per gram of BW. *H*: Quantification of the net area under curve of (*G*). *I*: Fasting blood glucose. Values in *B–I* are mean ± SD. $n = 5–9$ males and females. Age is 8–10 weeks. [#]$P < 0.05$ vs. *Nrf2*(f)[+/+]:*ob/ob* mice.

Ob/ob mice show enhanced adaptive antioxidant and inflammatory responses that are diminished by *Nrf2* deletion. GSH is the most important and abundant redox buffer in cells (21). By scavenging peroxides, mainly through glutathione peroxidase-catalyzed reactions, GSH oxidation forms GSSG. Key enzymes involved in the de novo synthesis and regeneration of GSH include glutamate cysteine ligase catalytic and regulatory subunit, GSH synthetase, and GSH reductase, which are all regulated, at least in part, by Nrf2 through the ARE (22–25). *Nrf2*^{+/+}: *ob/ob* mice expressed higher levels of *Gclm* and heme oxygenase 1 (*Ho1*) in WAT and *Gclc*, *Ho1*, and NAD(P)H: quinone oxidoreductase 1 (*Nqo1*) in liver than those in their non-*ob/ob* littermates (Fig. 4*A*; Supplementary Fig. 7). The absence of *Nrf2* in mice either on C57BL/6J or on *ob/ob* background showed a trend toward reduced expression

of these ARE genes. In addition, the expression of other antioxidant genes, such as superoxide dismutase 3 (*Sod3*), *Gpx2*, *Gpx4*, and thioredoxin reductase 1 *(Txnrd1)* displayed similar trends in WAT or liver (Supplementary Figs. 7 and 8), indicating *ob/ob* mice have enhanced adaptive antioxidant response that was diminished by *Nrf2* deletion. Compared with *Nrf2*^{+/+}:WT mice, *Nrf2*^{+/+}:*ob/ob* mice showed a trend toward increased whole-blood and plasma GSH and GSSG levels (Fig. 4*B* and Supplementary Fig. 9), which were reduced by ablation of *Nrf2*. These changes were greater for plasma than whole blood.

Inflammation is associated with many pathologies, including obesity and insulin resistance (26). *Nrf2*^{+/+}:*ob/ob* WAT showed a trend toward increased expression of several inflammatory response genes (Fig. 4*A*), including tumor necrosis factor α (*Tnfα*), interleukin 1β (*Il1β*), and
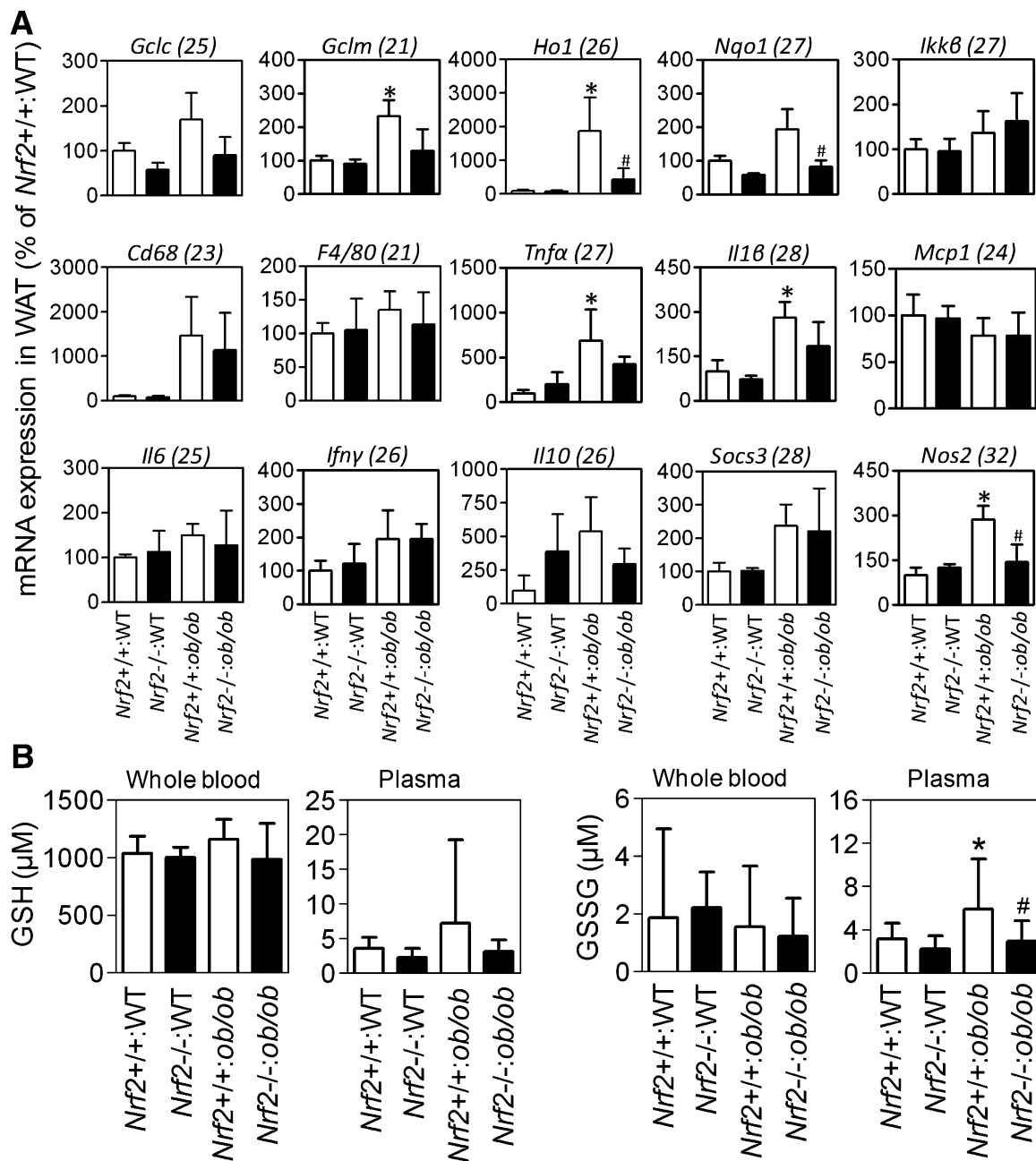
FIG. 4. *A*: mRNA expression of antioxidant and inflammatory response genes in epididymal WAT. *n* = 3–6 males. Animal age is 8–10 weeks. The number in brackets after each gene name is the Cq value of that gene in *Nrf2*$^{+/+}$:WT. The average Cq value of reference gene *18S* is 14. *B*: Glutathione levels in whole blood and plasma. GSH, reduced glutathione; GSSG, oxidized glutathione. *n* = 7–22. Animal age is 8–15 weeks. Values in (*A*) and (*B*) are mean ± SD. *$P < 0.05$ vs. non-*ob/ob* mice with the same Nrf2 genotype; #$P < 0.05$ vs. *Nrf2*$^{+/+}$:*ob/ob* mice.

nitric oxide synthetase 2 (*Nos2*) compared with *Nrf2*$^{+/+}$: WT mice, whereas the absence of *Nrf2* markedly diminished their induction. In addition, the mRNA expression of many antioxidant and inflammatory response genes in WAT trended lower in *Nrf2*(f)$^{-/-}$:*ob/ob* mice compared with *Nrf2*(f)$^{+/+}$:*ob/ob* mice (Supplementary Fig. 10).

Nrf2$^{-/-}$:ob/ob mice show insulin resistance in WAT, which displays impaired adipogenesis. To determine whether ablation of *Nrf2* in *ob/ob* mice results in insulin resistance in WAT, the key effecter of insulin signaling cascade, phosphorylated AKT (p-AKT), was determined in epididymal WAT of mice treated with insulin. Insulin-stimulated p-AKT(S473) and p-AKT(T308) in WAT of

Nrf2$^{-/-}$:*ob/ob* mice (Fig. 5*A* and *B*) were significantly lower than those in *Nrf2*$^{+/+}$:*ob/ob* mice, indicating reduced insulin sensitivity in WAT of *Nrf2*$^{-/-}$:*ob/ob* mice. To explore the mechanisms behind the insulin resistance in the WAT of *Nrf2*$^{-/-}$:*ob/ob* mice, mRNA expression profiling in epididymal WAT of *Nrf2*$^{-/-}$:*ob/ob* mice was determined by RT-qPCR. Because the metabolic phenotype of *Nrf2*$^{-/-}$: *ob/ob* mice was consistent for both males and females (Figs. 1 and 2 and Supplementary Figs. 2–6), mRNA expression profiling only was performed in one gender, the male mice. In addition to the induction of antioxidant and inflammatory response genes that was observed in *Nrf2*$^{+/+}$: *ob/ob* mice (Fig. 4*A* and Supplementary Fig. 8), the WAT of
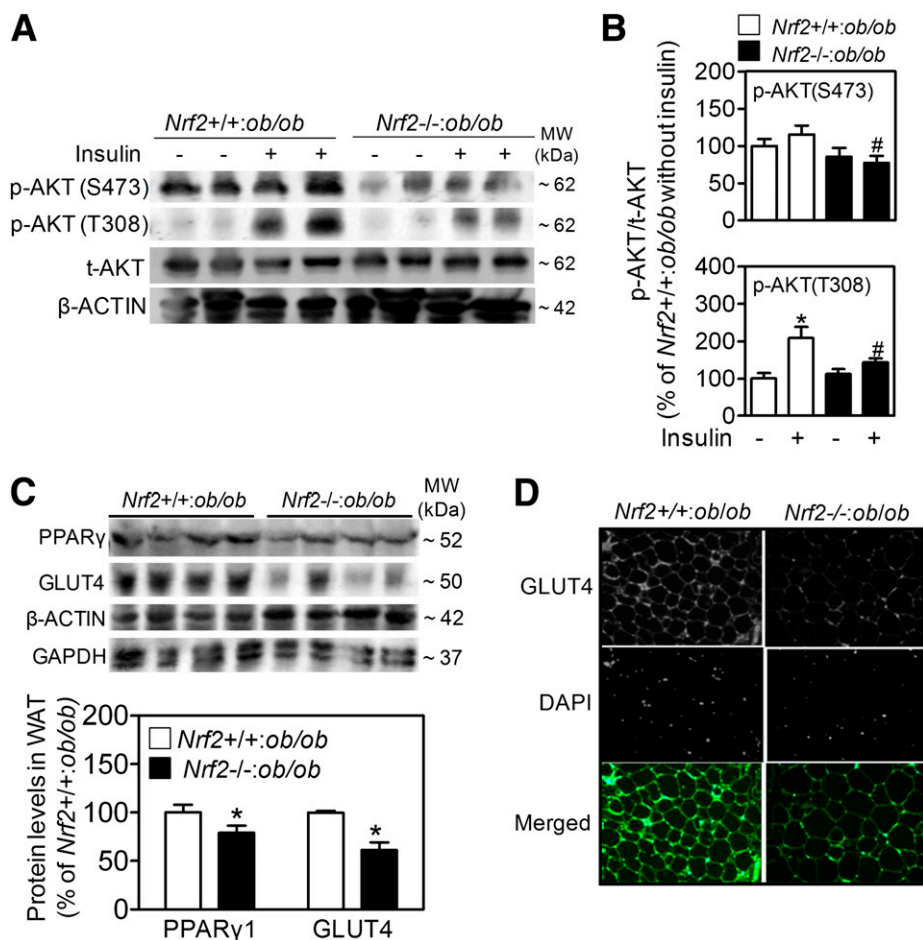
FIG. 5. *Nrf2⁻/⁻:ob/ob* mice show reduced protein expression of phosphorylated AKT, PPARγ, and GLUT4 in epididymal WAT. *A*: Representative images of immunoblots of phosphorylated AKT. WAT was collected after a 16-h fast with or without intraperitoneal insulin injection (4 U/kg BW; 15 min). β-Actin is a loading control. *B*: Quantification of immunoblotting of p-AKT(S473) and p-AKT(T308) normalized to total AKT (t-AKT). *n* = 4. **P* < 0.05 vs. *Nrf2⁺/⁺:ob/ob* mice without insulin; #*P* < 0.05 vs. *Nrf2⁺/⁺:ob/ob* mice with insulin. *C*: Representative images of immunoblots (upper panel) and quantification (lower panel) of PPARγ and GLUT4. *n* = 4. **P* < 0.05 vs. *Nrf2⁺/⁺:ob/ob* mice. *D*: Representative images of immunofluorescent staining of GLUT4. (A high-quality color representation of this figure is available in the online issue.)

Nrf2⁺/⁺:ob/ob mice trended higher levels of many genes related to adipogenesis (Supplementary Fig. 11) and lipogenesis (Supplementary Fig. 12), including *Pparγ2* and fatty acid synthetase (*Fas*), than levels in *Nrf2⁺/⁺* mice. The absence of *Nrf2* in *ob/ob* mice resulted in a trend toward reduced expression of most of these genes. In agreement with the findings in *Nrf2⁺/⁺:ob/ob* mice, *Nrf2(f)⁺/⁺:ob/ob* WAT also trended reduced levels of adipogenic and antioxidant response genes, including *Pparγ2*, adipose differentiation-related protein (*Adfp*), and *Fas* (Supplementary Fig. 13). In keeping with the reduced mRNA expression of adipogenic factors, the protein expression of PPARγ and GLUT4 in WAT of *ob/ob* mice also was significantly reduced by *Nrf2* deficiency (Fig. 5*C* and *D*).

DISCUSSION

WAT is pivotal to lipid homeostasis and energy balance and regulates the flux of fatty acids to peripheral tissues by storing and hydrolyzing triglyceride under hormonal control (1,27). Here, we show that on the *ob/ob* background, ablation of *Nrf2*, globally or specifically in adipocytes, results in reduced WAT mass but leads to an even more severe metabolic syndrome showing insulin resistance, hyperglycemia, and hyperlipidemia. It appears that the

extremely positive energy balance resulting from leptin deficiency uncovers a deleterious effect of *Nrf2* deletion in adipose tissues.

Adipogenesis is a complex process in which multipotent mesenchymal stem cells first become committed to fibroblast-like preadipocytes and subsequently convert to mature spherical adipocytes with lipid accumulation (28–31). Terminal adipogenesis involves a sequential cascade of gene expression events coordinated by transcription factors that simultaneously induce tissue-specific gene expression and repress alternate cell fates (29,30). At the center of this network is the adipogenic factor PPARγ, which orchestrates the entire terminal differentiation process (28–30). C/EBPs, including C/EBPα, C/EBPβ, and C/EBPδ, belong to basic leucine zipper transcription factors and are expressed in adipocytes (29). C/EBPβ and C/EBPδ are transiently expressed and function at an early stage of differentiation by sensing adipogenic stimuli and initiating the expression of PPARγ and C/EBPα (32). C/EBPα and PPARγ form a positive feedback loop and act at a later stage by inducing and maintaining expression of adipocyte-specific genes, including *Adfp*, *Fas*, *Cd36*, and *Glut4* (33). In the current study, many adipogenic genes exhibited a substantial increase in the WAT of *ob/ob* mice compared with non-*ob/ob* littermates. It appears that

adipogenesis contributes to the hypertrophy of WAT and weight gain of *ob/ob* mice. The results that $Nrf2^{-/-}$:*ob/ob* mice had fewer small adipocytes in WAT than $Nrf2^{+/+}$:*ob/ob* mice and that whole-body or adipocyte-specific ablation of *Nrf2* substantially reduced the expression of the adipogenic genes indicate that impaired adipogenesis occurred in the WAT of $Nrf2^{-/-}$:*ob/ob* mice. This finding is consistent with our previous studies showing that Nrf2 plays a critical role in adipogenesis by regulating the expression of C/EBPβ and PPARγ (11,12).

Extreme defects in adipogenesis (e.g., attributable to complete ablation of *Pparγ*) lead to lipodystrophy (34). However, less extreme reduction of adipogenesis alone does not cause lipodystrophy. For example, a moderate reduction in adipogenesis caused by PPARγ/RXR antagonists, heterozygous deficiency of *Pparγ*, or other genetic variants in *Pparγ* reduce adipose tissue mass without causing lipodystrophy (35–39). Although *Nrf2* plays important roles in regulating the expression of *Cebpβ* and *Pparγ*, the absence of *Nrf2* does not completely abolish PPARγ activity and adipogenesis (11,12). Thus, knocking-out of *Nrf2* reduces adipogenesis and also attenuates adipocyte hypertrophy and weight gain without causing an extreme reduction in adipose tissue mass (11,19). However, when adipose tissue expandability is limited by *Nrf2* deficiency on a hyperphagic *ob/ob* background, the excess energy intake cannot be stored adequately in the adipose tissues and, consequently, leads to ectopic lipid accumulation in circulation. This phenotype, observed in $Nrf2^{-/-}$:*ob/ob* and $Nrf2(f)^{-/-}$:*ob/ob* mice, is consistent with the manifestations of P465L PPARγ mutant or *Pparγ2*-knockout mice on an *ob/ob* background (20,40). It also suggests a synergistic interaction between *Nrf2* deletion and a severe positive energy balance caused by the lack of leptin in inducing severe metabolic syndrome. Considering the critical roles of adipogenesis in adipose formation and in keeping healthy adipose function, impairment of adipogenesis resulting from a deficiency in Nrf2 could contribute to a more severe metabolic syndrome in $Nrf2^{-/-}$:*ob/ob* and $Nrf2(f)^{-/-}$:*ob/ob* mice.

Oxidative stress, which is associated with many pathologies, including obesity and metabolic syndrome, can stem from a variety of sources, including overfeeding, high-fat diet, and exposure to certain environmental agents (41). Although potentially cytotoxic, reactive oxygen species (ROS) are important intracellular signaling molecules for cellular responses to a variety of physiological stimuli, including glucose sensing in pancreatic β cells (42) and insulin signal transduction in insulin-responsive cells (43). In adipose tissues, ROS promote the conversion from preadipocytes to mature adipocytes (12,44) and facilitate insulin action (43,45). These ROS-mediated biological signaling pathways could be adversely affected by enhanced Nrf2-ARE activity because ROS signaling intermediates should inversely correlate with the ROS-scavenging activity and antioxidant status in cells. When cells are chronically exposed to oxidative stressors, cellular ROS-scavenging capacity is adaptively upregulated, primarily through the activation of Nrf2 and subsequent transcriptional induction of a suite of antioxidant enzymes. The induced antioxidant enzymes, meant to maintain intracellular redox homeostasis and limit oxidative damage, may have the undesired effect of impeding the physiological role of ROS as signaling molecules. Thus, ROS, antioxidants, and the cellular adaptive antioxidant response seem to play counteracting roles in regulating adipose function.

Although antioxidants protect adipocytes from oxidative damage, they also may blunt aspects of ROS signaling, resulting in reduced adipogenesis and insulin resistance. In support of this idea, the absence of *Nrf2* in non-*ob/ob* mice resulted in a slightly leaner phenotype with increased insulin sensitivity (11,19). This lean phenotype might be associated with lowered antioxidant expression and improved ROS signaling. *Ob/ob* mice have elevated oxidative stress demonstrated by the increased levels of blood GSH and GSSG and induction of many Nrf2-target genes in WAT and the liver. Thus, Nrf2-mediated adaptive induction of antioxidant enzymes in *ob/ob* mice might account for their moderately reduced insulin sensitivity and glucose intolerance. The activation of Nrf2 in WAT of $Nrf2^{+/+}$:*ob/ob* mice also suggests that oxidative stress-triggered Nrf2 activation may be required for adipose accumulation. Because $Nrf2^{-/-}$:*ob/ob* mice show lowered antioxidant expression in WAT and the liver, we expected that the mice have enhanced ROS signaling and improved insulin sensitivity. However, an impaired insulin sensitivity and even more severe metabolic disorders were observed in both $Nrf2^{-/-}$:*ob/ob* and $Nrf2(f)^{-/-}$:*ob/ob* mice. This phenotype suggests that under challenge with extremely positive energy balance, the reduced capacity of WAT expansion is the dominant mechanism for their phenotype that cannot be fully compensated by enhanced ROS signaling from the Nrf2 deficiency.

Inflammation is involved in many aspects of the pathologies of obesity and metabolic syndrome (26). Nrf2-ARE signaling is involved in attenuating inflammation-associated pathogenesis (46). However, Nrf2 also is directly involved in the transcriptional regulation of proinflammatory cytokine *Il6* (47). Nrf2 deficiency attenuates high-fat diet-induced inflammation in the stromal vascular and adipocyte fractions of adipose tissues (43). Thus, there appears to be potential cross-talk between Nrf2-mediated antioxidant response and inflammatory response. In the current study, although inflammatory response was augmented in WAT of *ob/ob* mice and may be involved in their moderate insulin resistance, substantially reduced expression of many inflammation-related genes in WAT of $Nrf2^{-/-}$:*ob/ob* and $Nrf2(f)^{-/-}$:*ob/ob* mice indicated that their severe metabolic disorder is not attributable to inflammatory response.

In summary, our studies provide new insight into the mechanisms by which Nrf2 regulates adipose development and function. We found that Nrf2 controls WAT expandability and serves to maintain glucose and lipid homeostasis. Thus, this transcription factor, normally considered a regulatory protein for oxidative stress response, clearly has diverse roles, including control of adipogenesis. In addition, ROS, whose cellular concentrations decline with increases in Nrf2-regualted antioxidant gene expression, also affect insulin signaling. From our perspective, it has become increasingly clear that a full understanding of adipocyte function and obesity-associated metabolic disorders will require further investigations of the multiple interacting roles of Nrf2 in these physiological processes. In light of the involvement of Nrf2 in regulating adaptive antioxidant response and the association of metabolic syndrome with oxidative stress, we counsel caution in pursuing strategies to prevent or treat obesity and associated metabolic syndrome by manipulating Nrf2 function.

REFERENCES

1. Rosen ED, Spiegelman BM. Adipocytes as regulators of energy balance and glucose homeostasis. Nature 2006;444:847–853
2. Vigouroux C, Caron-Debarle M, Le Dour C, Magré J, Capeau J. Molecular mechanisms of human lipodystrophies: from adipocyte lipid droplet to oxidative stress and lipotoxicity. Int J Biochem Cell Biol 2011;43:862–876
3. Virtue S, Vidal-Puig A: Adipose tissue expandability, lipotoxicity and the metabolic syndrome–an allostatic perspective. Biochim Biophys Acta 2010;1801:338-349
4. Itoh K, Igarashi K, Hayashi N, Nishizawa M, Yamamoto M. Cloning and characterization of a novel erythroid cell-derived CNC family transcription factor heterodimerizing with the small Maf family proteins. Mol Cell Biol 1995;15:4184–4193
5. Kobayashi M, Yamamoto M. Nrf2-Keap1 regulation of cellular defense mechanisms against electrophiles and reactive oxygen species. Adv Enzyme Regul 2006;46:113–140
6. Thimmulappa RK, Lee H, Rangasamy T, et al. Nrf2 is a critical regulator of the innate immune response and survival during experimental sepsis. J Clin Invest 2006;116:984–995
7. Motohashi H, O'Connor T, Katsuoka F, Engel JD, Yamamoto M. Integration and diversity of the regulatory network composed of Maf and CNC families of transcription factors. Gene 2002;294:1–12
8. Itoh K, Mimura J, Yamamoto M. Discovery of the negative regulator of Nrf2, Keap1: a historical overview. Antioxid Redox Signal 2010;13:1665–1678
9. Cho HY, Reddy SP, Kleeberger SR. Nrf2 defends the lung from oxidative stress. Antioxid Redox Signal 2006;8:76–87
10. Itoh K, Chiba T, Takahashi S, et al. An Nrf2/small Maf heterodimer mediates the induction of phase II detoxifying enzyme genes through antioxidant response elements. Biochem Biophys Res Commun 1997;236:313–322
11. Pi J, Leung L, Xue P, et al. Deficiency in the nuclear factor E2-related factor-2 transcription factor results in impaired adipogenesis and protects against diet-induced obesity. J Biol Chem 2010;285:9292–9300
12. Hou Y, Xue P, Bai Y, et al. Nuclear factor erythroid-derived factor 2-related factor 2 regulates transcription of CCAAT/enhancer-binding protein β during adipogenesis. Free Radic Biol Med 2012;52:462–472
13. Garg A, Agarwal AK: Lipodystrophies: disorders of adipose tissue biology. Biochim Biophys Acta 2009;1791:507-513
14. Florenza CG, Chou SH, Mantzoros CS. Lipodystrophy: pathophysiology and advances in treatment. Nat Rev Endocrinol 2011;7:137–150
15. Chatterjee R, Bhattacharya P, Gavrilova O, et al. Suppression of the C/EBP family of transcription factors in adipose tissue causes lipodystrophy. J Mol Endocrinol 2011;46:175–192
16. Pi J, Bai Y, Daniel KW, et al. Persistent oxidative stress due to absence of uncoupling protein 2 associated with impaired pancreatic beta-cell function. Endocrinology 2009;150:3040–3048
17. Sajic T, Hopfgartner G, Szanto I, Varesio E. Comparison of three detergent-free protein extraction protocols for white adipose tissue. Anal Biochem 2011;415:215–217
18. Pi J, Qu W, Reece JM, Kumagai Y, Waalkes MP. Transcription factor Nrf2 activation by inorganic arsenic in cultured keratinocytes: involvement of hydrogen peroxide. Exp Cell Res 2003;290:234–245
19. Chartoumpekis DV, Ziros PG, Psyrogiannis AI, et al. Nrf2 represses FGF21 during long-term high-fat diet-induced obesity in mice. Diabetes 2011;60:2465–2473
20. Medina-Gomez G, Gray SL, Yetukuri L, et al. PPAR gamma 2 prevents lipotoxicity by controlling adipose tissue expandability and peripheral lipid metabolism. PLoS Genet 2007;3:e64
21. Schafer FQ, Buettner GR. Redox environment of the cell as viewed through the redox state of the glutathione disulfide/glutathione couple. Free Radic Biol Med 2001;30:1191–1212
22. McMahon M, Itoh K, Yamamoto M, et al. The Cap'n'Collar basic leucine zipper transcription factor Nrf2 (NF-E2 p45-related factor 2) controls both constitutive and inducible expression of intestinal detoxification and glutathione biosynthetic enzymes. Cancer Res 2001;61:3299–3307
23. Sekhar KR, Spitz DR, Harris S, et al. Redox-sensitive interaction between KIAA0132 and Nrf2 mediates indomethacin-induced expression of gamma-glutamylcysteine synthetase. Free Radic Biol Med 2002;32:650–662
24. Lee TD, Yang H, Whang J, Lu SC. Cloning and characterization of the human glutathione synthetase 5′-flanking region. Biochem J 2005;390:521–528
25. Thimmulappa RK, Mai KH, Srisuma S, Kensler TW, Yamamoto M, Biswal S. Identification of Nrf2-regulated genes induced by the chemopreventive agent sulforaphane by oligonucleotide microarray. Cancer Res 2002;62:5196–5203
26. Hotamisligil GS. Inflammation and metabolic disorders. Nature 2006;444:860–867
27. Czech MP. Fat targets for insulin signaling. Mol Cell 2002;9:695–696
28. Tontonoz P, Spiegelman BM. Fat and beyond: the diverse biology of PPARgamma. Annu Rev Biochem 2008;77:289–312
29. Rosen ED, MacDougald OA. Adipocyte differentiation from the inside out. Nat Rev Mol Cell Biol 2006;7:885–896
30. Farmer SR. Transcriptional control of adipocyte formation. Cell Metab 2006;4:263–273
31. Lefterova MI, Lazar MA. New developments in adipogenesis. Trends Endocrinol Metab 2009;20:107–114
32. Yeh WC, Cao Z, Classon M, McKnight SL. Cascade regulation of terminal adipocyte differentiation by three members of the C/EBP family of leucine zipper proteins. Genes Dev 1995;9:168–181
33. Wu Z, Rosen ED, Brun R, et al. Cross-regulation of C/EBP alpha and PPAR gamma controls the transcriptional pathway of adipogenesis and insulin sensitivity. Mol Cell 1999;3:151–158
34. Zhang J, Fu M, Cui T, et al. Selective disruption of PPARgamma 2 impairs the development of adipose tissue and insulin sensitivity. Proc Natl Acad Sci USA 2004;101:10703–10708
35. Yamauchi T, Waki H, Kamon J, et al. Inhibition of RXR and PPARgamma ameliorates diet-induced obesity and type 2 diabetes. J Clin Invest 2001;108:1001–1013
36. Rieusset J, Touri F, Michalik L, et al. A new selective peroxisome proliferator-activated receptor gamma antagonist with antiobesity and antidiabetic activity. Mol Endocrinol 2002;16:2628–2644
37. Kubota N, Terauchi Y, Miki H, et al. PPAR gamma mediates high-fat diet-induced adipocyte hypertrophy and insulin resistance. Mol Cell 1999;4:597–609
38. Miles PD, Barak Y, He W, Evans RM, Olefsky JM. Improved insulin-sensitivity in mice heterozygous for PPAR-gamma deficiency. J Clin Invest 2000;105:287–292
39. Deeb SS, Fajas L, Nemoto M, et al. A Pro12Ala substitution in PPAR-gamma2 associated with decreased receptor activity, lower body mass index and improved insulin sensitivity. Nat Genet 1998;20:284–287

40. Gray SL, Nora ED, Grosse J, et al. Leptin deficiency unmasks the deleterious effects of impaired peroxisome proliferator-activated receptor gamma function (P465L PPARgamma) in mice. Diabetes 2006;55:2669–2677

41. Furukawa S, Fujita T, Shimabukuro M, et al. Increased oxidative stress in obesity and its impact on metabolic syndrome. J Clin Invest 2004;114: 1752–1761

42. Pi J, Bai Y, Zhang Q, et al. Reactive oxygen species as a signal in glucose-stimulated insulin secretion. Diabetes 2007;56:1783–1791

43. Goldstein BJ, Mahadev K, Wu X, Zhu L, Motoshima H. Role of insulin-induced reactive oxygen species in the insulin signaling pathway. Antioxid Redox Signal 2005;7:1021–1031

44. Lee H, Lee YJ, Choi H, Ko EH, Kim JW. Reactive oxygen species facilitate adipocyte differentiation by accelerating mitotic clonal expansion. J Biol Chem 2009;284:10601–10609

45. Goldstein BJ, Mahadev K, Wu X. Redox paradox: insulin action is facilitated by insulin-stimulated reactive oxygen species with multiple potential signaling targets. Diabetes 2005;54:311–321

46. Kim J, Cha YN, Surh YJ. A protective role of nuclear factor-erythroid 2-related factor-2 (Nrf2) in inflammatory disorders. Mutat Res 2010;690: 12–23

47. Wruck CJ, Streetz K, Pavic G, et al. Nrf2 induces interleukin-6 (IL-6) expression via an antioxidant response element within the IL-6 promoter. J Biol Chem 2011;286:4493–4499